340287. CONVECTIVELY COUPLED EQUATORIAL KELVIN WAVES AND THEIR RELATIONSHIP WITH EASTERLY WAVES OVER THE INTRA AMERICAS SEAS AND EASTERN PACIFIC.

Victor M. Torres and Chris D. Thorncroft.
University at Albany. State University of New York. Albany, N.Y.

1. INTRODUCTION

Convectively coupled equatorial Kelvin Waves (CCEKWs) are eastward propagating features of the tropical atmosphere with phase speed of 15ms^{-1}, and periods of 3 to 15 days. Over the eastern Pacific, a region characterized by a warm pool, convection associated to CCEKWs shifts latitudinally over the northern hemisphere to around 10^{O}N (Straub and Kiladis 2002). It is also near this latitude, that Easterly Waves (EWs) are found over this basin.

Previous studies over Africa have shown that EW-activity increases during and after the passage of the convective phase of strong CCEKWs. This is because CCEKWs enhance convection, and provide a suitable environment for their further development (Ventrice and Thorncroft 2013). Over the Eastern Pacific, it has been documented that CCEKWs induce tropical cyclogenesis around 3.5 days after the CCEKW passage. Further analysis of rainfall suggests that EWs are involved in such processes (Schreck, 2015). Moreover, literature shows that the Madden-Julian oscillation (MJO) plays an essential role in modulating frequency and location of EWs as well as of tropical cyclones (Aiiyer and Molinari 2008, Rydbeck et al 2014).

While the existing literature has focused more on African EWs, and have ignored the relationship between CCEKWs and EWs over the eastern Pacific, we performed an analysis on this relationship and the environmental conditions that support EW growth. The following sections describe the data and methodology used for these goals and present results of the most important factors. The results show that CCEKWs in general do not induce genesis of EWs over the eastern Pacific, and that a larger-scale convective environment, such as the MJO, is necessary for genesis and further development.

2. DATA

We used data from ERA-Interim reanalysis (Dee et al. 2011) at 0.5º horizontal resolution at 28 vertical levels. For convection, NOAA OLR at 1º horizontal resolution was used and interpolated to 0.5º.

3. METHODOLOGY

This study considers the extended summer season of JJAS from 1980-2015.

CCEKWs are obtained by filtering according to Kiladis et al. (2009). After this, the region of maximum variability of CCEKWs over the IAS region and eastern Pacific was considered to be at 9ºN, 84ºW. Then at this point, linear regressions are performed as in Mekonnen et al. (2007), by using a Kelvin wave index like in Ventrice et al (Ventrice and Thorncroft 2013). For Easterly Wave activity, 2-10day filtered curvature vorticity at 850hPa is calculated and used as a metric.

To find the relationship between CCEKWs and EWs we create a Hovmoller methodology. Basically, this methodology consists of finding the dates when EWs had genesis while the convective phase of a CCEKW was present over the region of maximum CCEKW-variance. For this, OLR associated with CCEKWs was constrained to the band of 3º-12ºN, while for EWs this was between 6º-13ºN. These bands are considered given previous results for convection and EWs over the eastern Pacific. CCEKW-OLR are selected when their anomalies were under 0.5 standard deviation. Curvature vorticity, associated to EW,must exceed 0.1x10^{-5} s^{-1}. When both conditions are satisfied, a methodology analogous to Brammer and Thorncroft (2015) is used to identify EWs.

4. RESULTS

To have an overview of CCEKWS over the eastern Pacific and the IAS region, the regressed horizontal and vertical structure is shown in Fig. 1 at the selected point 9ºN, 84ºW. This figure shows OLR anomalies (Fig. 1.a and b), and 850 hPa streamfunction and winds (Fig. 1.b). At lag 0, enhanced convection is observed over the tropical eastern Pacific and Central America (Fig. 1.a and b). Ahead of negative streamfunction, significant westerlies impact the mountain regions of Central and South America.

* *Corresponding author address:* Victor M. Torres, SUNY-Albany DAES, Albany, NY 12222; e-mail: vtorrespuente@albany.edu.

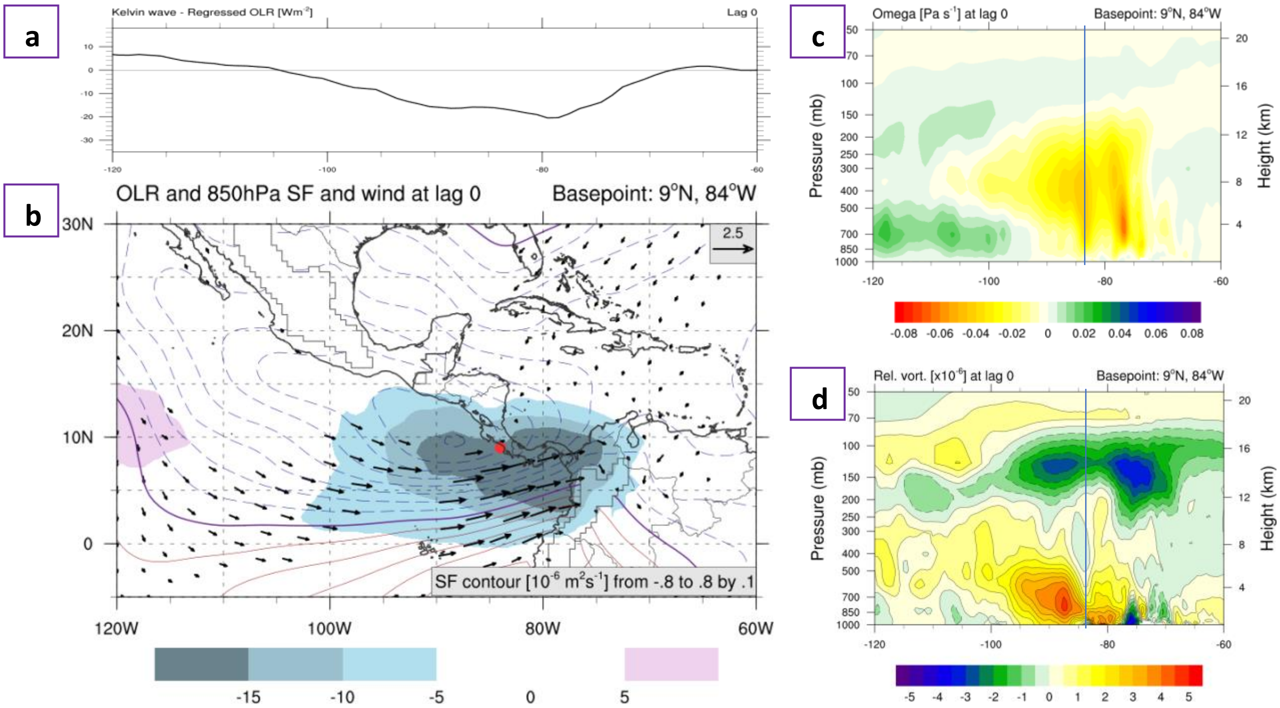

Figure 1. Horizontal and vertical structure of convectively coupled equatorial Kelvin waves during JJAS 1980-2015 at 9ºN, 84ºW (indicated by the red dot) on lag 0. **a.** OLR anomaly [Wm^{-2}] averaged between 7ºN-11ºN, **b.** OLR anomalies [Wm^{-2}] in shades, 850 hPa streamfunction [$x10^{-6}$ m^2s^{-1}] in contours (negative values are dashed), and winds [ms^{-1}]. **c.** Omega vertical velocity [$Pa\ s^{-1}$], and **d.** relative vorticity [$x10^{-5}$ s^{-1}] – anomalies along 9ºN. Vertical line indicates reference point at 84ºW. Data from NOAA Daily OLR TCDR at 0.5º resolution, and ERA-I at 0.5º resolution.

Convection is located north of the equator, where warm SSTs provide moist static energy to fuel deep convection, and over the equator, cold SSTs prevent deep convection from occurring.

Vertical cross sections of relative vorticity and vertical velocity omega of CCEKWs are shown in Figure 1.c and d. respectively. Each variable is averaged from 7ºN to 11ºN over the eastern Pacific to maximize the signature of these fields. Two peaks in vertical velocity (Fig. 1.c), at 84ºW and at 76ºW, suggests that convection associated with CCEKWs is found over Central America as well as over South America, and is greatly enhanced over the northern Andes. However, relative vorticity (Fig. 1.d) is only found over the eastern Pacific, close to the point of analysis and west of the Andes. This vorticity results from the development of cyclonic vorticity in the lower troposphere behind convection (Roundy 2008), and is essential for the downstream development of westward perturbations from the Central America region.

Considering that previous research used relative vorticity to study EWs over the Caribbean and eastern Pacific (Serra et al. 2008, 2011), we use curvature vorticity as an improved metric to identify EWs (Berry et al. 2007; Brammer and Thorncroft (2015)) over EKE (as in Ventrice and Thorncroft 2013), given that the latter could present spurious results.

Figure 2 shows Hovmoller diagrams of 2-10-day filtered curvature vorticity at 850hPa (shades) overlaid by CCEKW-OLR anomalies (contours) to show the relationship between CCEKWs and EWs. When considering all cases (Fig.2.a), positive curvature vorticity, from day -4 to day 0, moves along with the CCEKW-OLR envelope, however, at lag+1 we observe a westward propagation of negative curvature vorticity along with positive OLR. This result suggests that, in general, CCEKWs do not induce genesis of EWs over the eastern Pacific. When applying the methodology previously presented, the hovmoller diagram (Fig. 2.b) shows a very well defined peak of positive curvature vorticity at the time of the passage of a CCEKW. When compared to the same number of non-developing cases (randomly chosen), Fig. 2.c show similar features to that in Fig. 2.a, suggesting that EWs are not strong enough after CCEKW convective phase passage. However, given that in Fig. 2.b shows positive curvature vorticity e.g., at lag -7, other large-scale synoptic phenomena like MJO are explored.

Figure 3 shows the partition of the relationship of CCEKW-EWs previously found

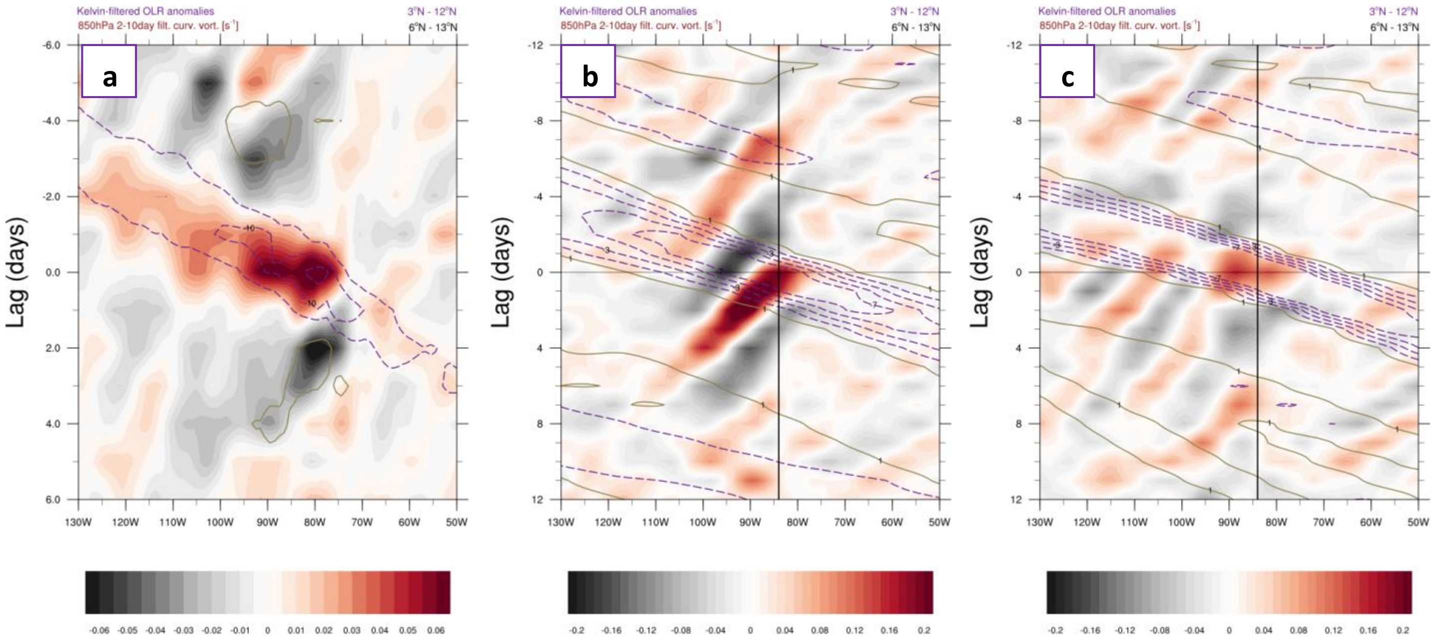

Figure 2. Time-longitude composite of daily averaged 850 hPa 2-10-day filtered curvature vorticity (shades) averaged over each CCEKW between 6ºN-13ºN, and Kelvin filtered OLR anomalies are averaged between 3ºN-12ºN **a.** For all cases, **b.** For EWs developing from CCEKWs following the methodology, and **c.** For 40 random cases. Negative Kelvin filtered OLR anomalies are dashed, while positive OLR anomalies are continuous. Shade interval is $5x10^{-5}$ s^{-1}; contour intervals are 5 Wm^{-2}. Vertical line indicates reference point at 84ºW. Data from NOAA Daily OLR TCDR at 0.5º resolution, and ERA-I at 0.5º resolution.

(Fig. 3.a) during MJO convective (Fig. 3.b) and MJO non-convective (Fig. 3.c) phases. When the MJO convective phase is present, it is very clear that the MJO helps to trigger EWs over the region. In particular, when CCEKWs are present within the MJO environment, CCEKWs enhance curvature vorticity associated with westward propagating EWs, in agreement with previous studies (Aiiyer and Molinari 2008, Shreck 2015). In comparison, during MJO non-convective phases, curvature vorticity associated with EWs is short-lived and not as intense as during convective events.

5. CONCLUSIONS

This study shows the basic structure of CCEKWs over the eastern Pacific and IAS region. From this, we can observe that after the convective passage of a CCEKW, suppression of convection, and negative curvature vorticity follows. In general, CCEKWs do not induce EW genesis over the eastern Pacific, and only about a 20% of CCEKWs result in EW genesis. Furthermore, a larger-scale convective environment, such as the MJO is necessary for genesis and further development.

By recognizing that the MJO plays a fundamental role in the genesis of EWs over the eastern Pacific and IAS region, we show that EWs resulting from CCEKWs during convective MJO phases were more intense and propagate for a longer time when compared with those during non-convective MJO phases, which are the minority of the cases.

These results extend those of Aiyyer and Molinari (2008) and complete those of Schreck (2015) for CCEKW-genesis and the role of the MJO on EWs over the eastern Pacific.

REFERENCES

Aiyyer, A., and J. Molinari, 2008: MJO and Tropical Cyclogenesis in the Gulf of Mexico and Eastern Pacific: Case Study and Idealized Numerical Modeling. J. Atmos. Sci., 65, 2691-2704.

Berry, G., C. Thorncroft, and T. Hewson, 2007: African easterly waves during 2004-Analysis using objective techniques. Mon. Wea. Rev., 135, 1251-1267.

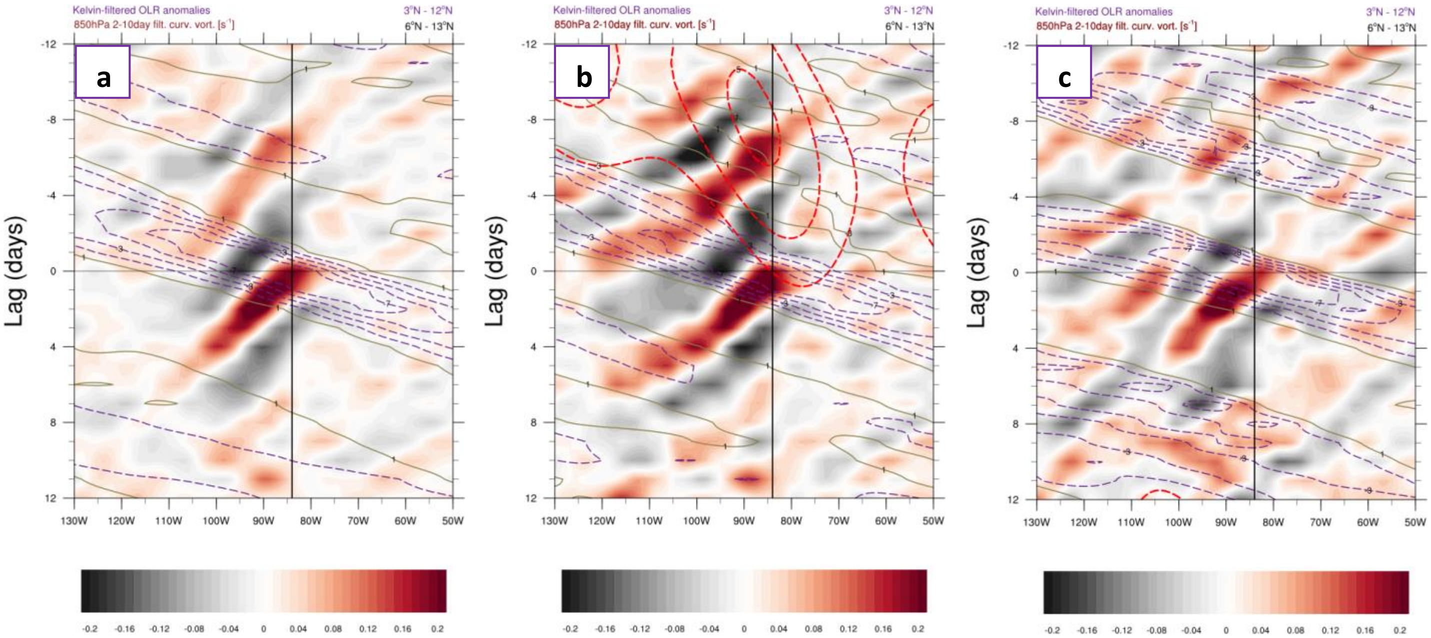

Figure 3. Time-longitude composite of daily averaged 850 hPa 2-10-day filtered curvature vorticity (shades) averaged over each CCEKW between 6ºN-13ºN, and Kelvin filtered OLR anomalies are averaged between 3ºN-12ºN **a.** For all EWs developing from CCEKWs, **b.** For cases during MJO 8-1-2 phases, and **c.** For cases during MJO 4-5-6 phases. Negative Kelvin filtered OLR anomalies are dashed, while positive OLR anomalies are continuous. Shade interval is $5x10^{-5}$ s^{-1}; contour intervals are 5 Wm^{-2}. Vertical line indicates reference point at 84ºW. Data from NOAA Daily OLR TCDR at 0.5º resolution, and ERA-I at 0.5º resolution.

Brammer, A., and C. D. Thorncroft, 2015: Variability and Evolution of African Easterly Wave Structures and the Relationship with Tropical Cyclogenesis over the Eastern Atlantic. Mon. Wea. Rev.

Dee, D. P., and Coauthors, 2011: The ERA-Interim reanalysis: configuration and performance of the data assimilation system. Quart. J. Roy. Meteor. Soc., 137, 553-597.

Kiladis, G. N., M. C. Wheeler, P. T. Haertel, K. H. Straub, and P. E. Roundy, 2009: Convectively coupled equatorial waves. Rev. Geophys., 47.

Mekonnen, A., C. D. Thorncroft, and A. R. Aiyyer, 2006: Analysis of convection and its association with African easterly waves. J. Climate, 19, 5405-5421.

Roundy, P. E., 2008: Analysis of convectively coupled Kelvin waves in the Indian Ocean MJO. J. Atmos. Sci., 65, 1342-1359.

Rydbeck, A. V., and E. D. Maloney, 2014: Energetics of East Pacific Easterly Waves during Intraseasonal Events. J. Climate, 27, 7603-7621.

Schreck, C. J., 2015: Kelvin Waves and Tropical Cyclogenesis: A Global Survey. Mon. Wea. Rev., 143, 3996-4011.

Serra, Y. L., G. N. Kiladis, and M. F. Cronin, 2008: Horizontal and vertical structure of easterly waves in the Pacific ITCZ. J. Atmos. Sci., 65, 1266-1284.

Serra, Y. L., G. N. Kiladis, and K. I. Hodges, 2010: Tracking and Mean Structure of Easterly Waves over the Intra-Americas Sea. J. Climate, 23, 4823-4840.

Straub, K. H., and G. N. Kiladis, 2002: Observations of a convectively coupled Kelvin wave in the eastern Pacific ITCZ. J. Atmos. Sci., 59, 30-53.

Ventrice, M. J., and C. D. Thorncroft, 2013: The Role of Convectively Coupled Atmospheric Kelvin Waves on African Easterly Wave Activity. Mon. Wea. Rev., 141, 1910-1924.